Exclusive quasifree pion photoproduction on complex nuclei in the Δ region

Xiaodong Li and L. E. Wright
Institute of Nuclear and Particle Physics, Physics Department, Ohio University, Athens, Ohio 45701

C. Bennhold
Department of Physics, Center of Nuclear Studies, The George Washington University, Washington, DC 20052
(Received 10 November 1992)

We present an analysis of the reaction $A(\gamma,\pi N)B$ in the full distorted wave impulse approximation carried out in momentum space. The bound nucleon is in a single particle orbital while the outgoing pion and nucleon are described by appropriate optical potential wave functions. The pion photoproduction operator of Blomqvist and Laget is used. This reaction allows for more direct studies of Δ properties in the nuclear medium than the reaction $A(\gamma,\pi)B$ since the final nucleon is no longer bound and the sensitivity to the nuclear structure of the target is thereby largely reduced. Kinematically, the reaction provides a great deal of flexibility because the target can take up a wide range of momentum transfer and little energy. Our calculations agree roughly with data from Tomsk but overestimate data from Bates. Nonlocal effects tend to enhance the local cross sections and in some cases are significant. For future experiments we propose kinematics that greatly reduce uncertainties from the optical potentials and expose information from the production vertex. We find that photon asymmetry contains such information in the cleanest way and it should be pursued. We suggest forward pion angles where discrepancies between data and theory exist should be studied more carefully by experiments.

PACS number(s): 25.20.Lj, 13.60.Le, 13.60.Rj

I. INTRODUCTION

For a number of years the Δ(3,3) resonance has been recognized as an important non-nucleonic degree of freedom for nuclear physics at intermediate energies. As the first excited state of the nucleon at $E = 1232$ MeV it was first observed in π^+p scattering with the large cross section of around 100 mb. The photon excites a nucleon to a delta primarily through a $M1$ transition, flipping the spin of one of the quarks inside the nucleon. Even though photon-induced reactions are intrinsically much weaker than pion-induced processes and can therefore sample the entire nuclear volume, the total photoabsorption cross section on a nucleus A is not simply given by $\sigma_{\gamma A} \approx A\,\sigma_{\gamma N}$ [1]. This is partly caused by kinematical effects like the smearing of the Δ resonance due to nucleon Fermi motion but it may also partly be caused by dynamical effects related to the ΔN interaction.

In the past, information on the Δ-nucleus interaction could only be extracted indirectly from reactions like pion elastic and inelastic scattering, and pion photoproduction on nuclei. In descriptions like the Δ-hole model, the delta is treated as an explicit degree of freedom whose propagation in the nucleus is modified by the surrounding medium. These medium corrections are introduced by including terms in the delta propagator that prevent the delta from decaying into Pauli-blocked states and account for coherent multiple scattering of the pion [2]. Furthermore, a phenomenological spreading protential has been included which can be related to an effective two-body Δ-N interaction. Including this Δ-N interaction explicitly was important in successfully reproducing recent data of $(\pi^\pm,\pi^\pm p)$ and $(\pi^+,\pi^0 p)$ reactions on ^{16}O [3]. It was found that the forward-backward ratio of quasifree $(\pi,\pi' N)$ cross sections is significantly modified by Δ medium modifications indicating the importance of the Δ-nucleus interaction in this energy region.

Pion photoproduction from p-shell nuclei with the reaction $A(\gamma,\pi)B$ where B is in a well-defined state (usually the ground state) has been extensively studied both theoretically and experimentally over the past decade. Much of this work has recently been reviewed in Ref. [4], where one can find most of the references. In addition, a summary of low-energy charged pion production from p-shell nuclei is given in Ref. [5]. The distorted wave impulse approximation (DWIA) analysis of this reaction has been fairly successful in analyzing most charged pion photoproduction experiments [5–9]. However, in the case of the reaction $^{14}\mathrm{N}(\gamma,\pi^+)^{14}\mathrm{C}_{\mathrm{g.s.}}$ large discrepancies were observed between data [10] and theoretical calculations at the higher energies of E_γ=260 and 320 MeV. Only after properly including unitarity in the elementary operator and a pion wave function generated by the Δ-hole model as done in Ref. [11] could these disagreements be partly reduced. Reference [7] obtained similar results in a combined DWIA and Δ-hole calculation. Since this reaction requires the final nucleon to remain bound in the residual nucleus, the calculations are very sensitive to

the nuclear transition structure of the target which may obscure the process of primary interest: pion photoproduction in the medium. However, the sensitivity to the nuclear transition matrix elements can be removed by allowing the final nucleon produced in the pion production process to exit the nucleus.

In this paper we investigate the exclusive reaction $A(\gamma,\pi N)B$ in the Δ resonance region, and as in (γ,π) experiments are primarily interested in cases where B is in its ground state or other low-lying state. By measuring in coincidence the momenta of the pion and the nucleon, the decay products of the Δ, one can in some sense measure Δ production in the nucleus. Thus the reaction cross section and polarization observables in principle contain information on the medium modification of the Δ. The nucleus just provides a scattering chamber which may modify the properties of the particles in it. Computations such as these could then be contrasted with explicit (γ,Δ) knock-out calculations, in which the Δ is produced and knocked out, interacting with the residual nucleus via a Δ-nucleus optical potential. In the long run one might want to use the $(\gamma,\pi N)$ reaction to verify if there are preformed Δ components in the nuclear many-body wave function. While such calculations are a long way off for p-shell nuclei, they have already been performed for very light nuclei such as ^{3}He and a Δ content of 1–2 % has been found in the nuclear wave function. Experiments involving the $(e,e'\pi N)$ reaction have been proposed to verify this prediction. In this paper, we only consider complex nuclei with mass number $A > 10$ where an optical potential description for the outgoing pion and nucleon is appropriate. Few-body systems require a different formalism than the one employed below.

Extensive studies of quasifree pion photoproduction and photoabsorption were performed by Oset and collaborators [12]. In their work great care was taken to properly and consistently include the modifications of the πN interactions by the surrounding nuclear medium. However, their investigation was performed in a nuclear matter framework followed by a local density approximation in order to compare with data for a particular nucleus. While this theoretical framework yielded good results for inclusive reactions where final states are not resolved and thus integrated over, the exclusive $(\gamma,\pi N)$ process is sensitive to single particle nucleon wave function and, therefore, requires a finite nucleus calculation.

Encouraged by the success of the DWIA approach in the analysis of the $A(\gamma,\pi)B$ reaction, our goal is to set up a nonlocal DWIA formalism for the $A(\gamma,\pi N)B$ reaction using the same standard physics inputs. Such a calculation is timely since there already exist a few experiments for the reaction [13–15] and more with better quality are expected in the near future. Even though previous calculations on $A(\gamma,\pi)B$ [5–7, 11] and inclusive quasifree $A(\gamma,\pi)X$ reactions were all performed in a nonlocal framework, no nonlocal computations have been performed for exclusive $A(\gamma,\pi N)B$ processes. The theoretical results available up to now [13–16] employ a factorized impulse approximation suggested by Laget [17]. Following the analogous development of $A(\gamma,\pi)B$ calculations we find it important to assess the significance of nonlocal effects. The additional nucleon in the final state adds new computational challenges because additional partial waves need to be summed over. Experimentally, the reaction poses challenges too because the final nuclear state, the outgoing pion and nucleon all need to be identified in coincidence with sufficient energy resolution and solid angle coverage. At the present stage, we neglect possible medium modifications and only use the free production amplitudes, to see if there are significant deviations of experiments from our nonlocal DWIA description. If such deviations are found, then more sophisticated calculations involving coupled channels or the Δ-hole model [2, 18] are called for.

Data for the exclusive reaction on complex nuclei in the Δ region are sparse. There is a recent review article by Van der Steenhoven [16] which summarizes the experimental situation to date. A number of experiments on ^{12}C have been done at the Tomsk synchrotron [13, 14], and an experiment on ^{16}O has been done at MIT Bates [15]. Recently, another experiment on ^{12}C has been completed at MIT Bates [19], but it is beyond the Δ region and we will not discuss it in this paper. In the case of the Bates experiment in the Δ region, the statistics are poor and error bars are large, and the coincidence cross section was integrated over the pion energy thus making it not truly exclusive. The Tomsk experiment suffers from a not-well-defined photon beam. With the advent of improved or new high duty cycle accelerators such as LEGS at Brookhaven, CEBAF, Bates, NIKHEF, and MAMI, and with better resolution and particle detection techniques, more accurate data should become available in the near future. The understanding of such data will greatly enhance our knowledge of many aspects of pion photoproduction from complex nuclei. In fact, there has recently been an approved proposal by Hicks [20] to measure cross sections and photon asymmetries on ^{12}C using the LEGS facility at Brookhaven. The preparation work on the experiment is ongoing and we are providing theoretical support. Also, NIKHEF is planning to do the exclusive experiments on ^{12}C and ^{4}He [16].

II. MODEL INGREDIENTS

Figure 1 is a diagrammatic illustration of this reaction in DWIA: a photon penetrates the nucleus and interacts with a single bound nucleon and excites a delta, the delta propagates inside the nucleus resulting in the emission of a pion and a nucleon which interact with the remaining

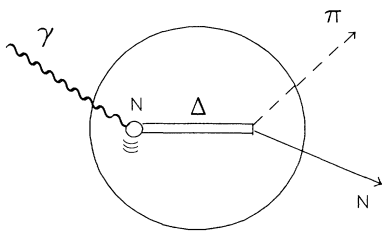

FIG. 1. Diagram of the reaction $A(\gamma,\pi N)B$ in the Δ region. The background Born terms are not shown.

nucleons while leaving the nucleus. When the photon energy reaches above 300 MeV the delta contribution becomes significant, approximately equal to the background contribution arising from the Born terms in the case of charged pions, completely dominant in the case of neutral pions. The following basic ingredients are needed in such a calculation: (1) single nucleon bound wave functions and associated spectroscopic factors, (2) elementary pion photoproduction operator, and (3) pion and nucleon optical potentials. As an initial step we use harmonic oscillator wave functions to describe the bound nucleon and since we are interested in the low-momentum-transfer region, they should be adequate. The spectroscopic factor is defined as the overlap between the initial nucleus with a nucleon removed and the final nuclear state. We use the values determined in $(e, e'p)$ experiments and in case we are examining a neutron assume it is equal to the proton. For example, a value of 3.6 is used for the $1p$ shell in ^{16}O, while 2.6 is used for the $p_{3/2}$ shell in ^{12}C. The spectroscopic factor only affects the overall normalization of the cross section, and thus does not enter polarization observables.

For the pion photoproduction process, we use the full Blomqvist-Laget (BL) production operator [21, 22] along with the second $\gamma N\Delta$ coupling in the Δ channel [23] without the various approximations that were made in earlier versions of the operator. The operator is expressed in an arbitrary frame of reference which makes it convenient for use in nuclear calculations where the struck nucleon has a distribution of momentum. We use the nonrelativistic reduction of the operator valid to order $(p/m)^2$ since relativistic effects were found to be small [5]. Actually only the vertex operators, nucleon and Δ spinors and the numerators of the propagators were evaluated to order $(p/m)^2$, whereas the full relativistic form was kept for the denominators of the propagators. The operator was unitarized by introducing appropriate complex phases in the amplitudes. The BL amplitudes describe the elementary pion photoproduction data reasonably well over a wide range of energies. We have decomposed the operator into spin 0 and spin 1 parts for the different elementary processes. The full expressions with the Born terms and the $\Delta(1232)$ resonance terms written out separately are given in the Appendix. We note that other models for pion photoproduction have recently emerged; one is by Davidson, Mukhopadhyay, and Wittman (DMW) [24], another is by Nozawa, Blankleider, and Lee (NBL) [25]. In a recent experiment done at LEGS [26] for the elementary process $p(\vec{\gamma}, \pi^0)$ in the Δ region, both of these models were compared with the photon polarization data. We have examined the same data using the BL amplitudes and find results similar to those obtained using the NBL amplitudes. In future studies we will make a comparison of these different models using the exclusive reaction from complex nuclei.

For the pion optical potential, we use the one developed by the group of Stricker, McManus, and Carr by solving the Klein-Gordon equation [27]. Their analyses give good fits to low-energy data for pionic atom data, nuclear absorption cross sections, and pion-nucleus elastic scattering cross sections. At higher pion energies (up to 220 MeV) they give an extrapolation of the optical potential parameters which also gives satisfactory agreements with experimental data. This covers the pion energy range in our calculations. As found in earlier work [6, 15] and in our investigations here, for exclusive reaction the pion optical potential primarily furnishes an overall reduction of the cross section for a given pion energy. Optical potentials which fit elastic scattering reasonably well can serve as a starting point for the exclusive reaction; however, with more precise data this reaction might distinguish among phase equivalent potentials. Furthermore, as we discuss later, the photon asymmetry is almost independent of the nucleon or pion distortions.

For the nucleon optical potential, many models exist in the literature. Most do a good job fitting the data. In the region we are interested in, the kinetic energy of the nucleon is generally below 200 MeV, so a nonrelativistic optical model for the nucleon is sufficient. We choose a global phenomenological potential by Schwandt *et al.* [28]. Both analyzing power data and cross section data were used to constrain the parameters.

Perhaps we should emphasize here that the calculation is set up in a rather general way so that each ingredient can be replaced by an alternative one. As data accumulate, we will look into each ingredient and fine-tune the calculation to meet the level of experimental accuracy.

III. DWIA FORMALISM

A. Kinematic considerations

In this section we define the coordinate system in the laboratory frame and briefly discuss the kinematic aspect of the reaction. Let the four-momenta of the photon, struck nucleon, pion, and outgoing nucleon be $k^\mu = (E_\gamma, \mathbf{k})$, $p_i^\mu = (E_{p_i}, \mathbf{p}_i)$, $q^\mu = (E_\pi, \mathbf{q})$, $p^\mu = (E_N, \mathbf{p})$, respectively. The target is at rest. The incoming photon beam defines the z axis while the pion is produced in the x-z plane with $\phi_\pi = 0°$. The momenta of the outgoing nucleon and residual nucleus are in general not constrained to lie in the production plane. Overall energy and momentum conservation gives

$$E_\gamma + M_i = E_\pi + E_N + M_f + T_Q, \tag{1}$$

$$\mathbf{k} = \mathbf{q} + \mathbf{p} + \mathbf{Q}, \tag{2}$$

where M_i and M_f are the rest mass energies of the initial and final nuclei and T_Q is the kinetic energy of the recoiling nucleus (small). Also $E_\gamma = |\mathbf{k}|$ since we deal with real photons and $E_\pi = (q^2 + m_\pi^2)^{1/2} = T_\pi + m_\pi$ and $E_N = (p^2 + m_N^2)^{1/2} = T_N + m_N$. Another kinematic quantity that is useful in describing the reaction is the invariant mass of the outgoing πN pair $W = \sqrt{(p^\mu + q^\mu)^2}$ which relates the nuclear results to the free production process. In the impulse approximation, the momentum of the struck nucleon is equal to the negative of the momentum transfer, $\mathbf{p}_i = -\mathbf{Q}$. Sometimes $\mathbf{p}_i$ is also called the missing momentum. One can see from Eqs. (1) and (2)

that the presence of the nucleus relaxes the rigid kinematic relations between the momenta of the pion and nucleon as found in the reaction on a free nucleon since the recoiling nucleus can take up various amounts of momentum transfer and very little energy compared to its mass. We can neglect its speed and let it generate optical potentials at the origin of the laboratory frame. The momentum transfer can range from zero up as compared to the $A(\gamma,\pi)B$ reaction where the minimum momentum transfer is about 140 MeV/c (pion rest mass). In this paper we are primarily interested in the quasifree region where the momentum transfer is relatively low (below 300 MeV/c). This will remove any strong dependence on the details of the single particle nuclear wave functions, and will also result in larger cross sections. Higher momentum transfer regions, on the other hand, can be used to map out single nucleon wave functions.

In order to concentrate on the basic production process, one wants to keep the influence of other ingredients in the calculation as constant as possible, and the kinematic flexibility in this reaction can help in this regard. Consider the following simple kinematic conditions where we restrict ourselves to coplanar geometry for simplicity. We specify E_γ, Q, T_π, θ_π, and $\phi_N = 180°$ in Eqs. (1) and (2), and solve for T_N, θ_N, θ_Q, and ϕ_Q. In this way, the lengths of all external momenta ($\mathbf{k}$, $\mathbf{p}$, $\mathbf{q}$, and $\mathbf{Q}$) are fixed; therefore the effects of final-state interaction and the magnitude of the momentum transfer to the recoiling nucleus are kept constant. Meanwhile, the pion and nucleon angles can be varied to obtain an angular distribution which depends sensitively on the basic production operator. Of course the distortions from pion and nucleon optical potentials still influence the cross section, but they are evaluated at the same energy over the complete angular range. We will present some results using this kinematic condition in Sec. IV C.

B. Differential cross section

Following standard procedures, the coincidence differential cross section for $A(\gamma,\pi N)B$ in the laboratory frame can be written as

$$\frac{d^3\sigma}{dE_\pi\, d\Omega_\pi\, d\Omega_N} = \frac{M_f m_N\, q\, p}{4(2\pi)^5 E_\gamma |E_N + E_f - E_N\, \mathbf{p}\cdot(\mathbf{k}-\mathbf{q})/p^2|}\ \overline{\sum}|M_{fi}|^2, \tag{3}$$

where $\overline{\sum}$ means sum over final spins and average over initial spins. For those facilities which have the capabilities of producing polarized photon beams, we introduce another observable Σ called the photon asymmetry. It is defined as

$$\Sigma = \frac{d^3\sigma_\perp - d^3\sigma_\parallel}{d^3\sigma_\perp + d^3\sigma_\parallel}, \tag{4}$$

where $\perp$ and $\parallel$ are the perpendicular and parallel photon polarization relative to the production plane (x-z plane). In the impulse approximation the matrix element in Eq. (3) reduces to a sum over single particle matrix element given by

$$\overline{\sum}|M_{fi}|^2 = \frac{1}{2(2J_i+1)} \sum_{\alpha\,\lambda\, m_s} \frac{S_\alpha}{2j+1}\, |\,T(\alpha,\lambda,m_s)\,|^2, \tag{5}$$

where J_i is the spin of the target, $\alpha = \{nljm\}$ is the quantum number of the bound nucleon, λ is the photon polarization, m_s is the spin projection of the outgoing nucleon, and S_α is the spectroscopic factor. The single particle matrix element T is given by

$$T(\alpha,\lambda,m_s) = \int d^3r\, \Psi^{(+)}_{m_s}(\mathbf{r},-\mathbf{p})\, \phi^{(+)}_\pi(\mathbf{r},-\mathbf{q})\, t_{\gamma\pi}(\lambda,\mathbf{k},\mathbf{p}_i,\mathbf{q},\mathbf{p})\, \Psi_\alpha(\mathbf{r})\, e^{i\mathbf{k}\cdot\mathbf{r}}, \tag{6}$$

where $\mathbf{p}_i = \mathbf{p} + \mathbf{q} - \mathbf{k}$ is the momentum of the bound nucleon. The partial wave expansions are

$$\Psi_\alpha(\mathbf{r}) = \sum_{m_l\, m_s^i} C^{l\ 1/2\ j}_{m_l\ m_s^i\ m}\, \phi_\alpha(r)\, Y^l_{m_l}(\hat{\mathbf{r}})\, \chi_{m_s^i}, \tag{7}$$

$$\phi^{(+)}_\pi(\mathbf{r},-\mathbf{q}) = \sum_{l_\pi} (-i)^{l_\pi}\, (2l_\pi+1)\, U_{l_\pi}(r,q)\, P_{l_\pi}(\hat{\mathbf{r}}\cdot\hat{\mathbf{q}}), \tag{8}$$

$$\Psi^{(+)}_{m_s}(\mathbf{r},-\mathbf{p}) = 4\pi \sum_{\substack{\kappa_p\, m_p \\ m_l'\, m_s'}} (-i)^{l_p} U_{\kappa_p}(r,p)\, C^{l_p\ 1/2\ j_p}_{m_l'\ m_s\ m_p}\, C^{l_p\ 1/2\ j_p}_{m_l'\ m_s'\ m_p}\, Y^{l_p}_{m_l'}(\hat{\mathbf{p}})\, Y^{l_p *}_{m_l'}(\hat{\mathbf{r}})\, \chi^\dagger_{m_s'}, \tag{9}$$

where the index $\kappa_p = \{j_p, l_p\}$. Also $\chi_{m_s^i}$ and $\chi_{m_s'}$ are the Pauli spinors for the bound nucleon and the outgoing nucleon respectively. The pion production operator $t_{\gamma\pi}$ is given in the Appendix. This production operator depends strongly on the momenta of the four particles involved at the vertex. In configuration space, momenta are gradients $\mathbf{p} \to -i\nabla_p$, $\mathbf{q} \to -i\nabla_q$ and they operate on the corresponding wave functions. Thus the operator is nonlocal. Such nonlocalities have been found to be important in explaining pion photoproduction data [5–7]. Usually they are difficult to handle in configuration space because the gradients appear in the operator in a very complicated way. So various approximations were made. To circumvent this problem, we choose to work in momentum space where the matrix element in Eq. (6) is given by a six-dimensional integral

$$T(\alpha,\lambda,m_s) = \int d^3p'\, d^3q'\, \Psi^{(+)}_{m_s}(\mathbf{p}',\mathbf{p})\, \phi^{(+)}_{\pi} \times(\mathbf{q}',\mathbf{q})\, t_{\gamma\pi}(\lambda,\mathbf{k},\mathbf{p}_i,\mathbf{q}',\mathbf{p}')\, \Psi_\alpha(\mathbf{p}_i) \tag{10}$$

with $\mathbf{p}_i = \mathbf{p}' + \mathbf{q}' - \mathbf{k}$. Here we can use the momentum space wave functions that either are directly available or are obtained from their configuration space counterparts by Fourier transforms. Working in momentum space allows a straightforward treatment of all nonlocal effects arising from the production operator without any approximation. However, the price we pay is the evaluation of a six-dimensional integral which requires considerable computations.

We now address the off-shell treatment of the basic production operator when embedding it into the nucleus. In order to avoid singularities in the propagators (particularly in the pion pole term) we place the pion and the final nucleon on their mass shell in the basic operator: $E_\pi'^{\,2} = q'^2 + m_\pi^2$ and $E_N'^{\,2} = p'^2 + m_N^2$. The energy of the bound nucleon is then given by $E_{p_i} = E_\pi' + E_N' - E_\gamma$, which in general makes the bound nucleon off-shell ($E_{p_i}^2 \neq p_i^2 + m_N^2$). Note that the outgoing pion and nucleon energies in the remainder of the kinematics are given by their asymptotic values.

At this point, it is useful to discuss some approximations that are commonly made. Firstly, in Eq. (10) if we fix the intermediate pion and proton momenta $\mathbf{q}'$ and $\mathbf{p}'$ at their asymptotic values $\mathbf{q}$ and $\mathbf{p}$, i.e., we make the production operator $t_{\gamma\pi}$ local, then the matrix element reduces to a three-dimensional integral [see Eq. (6)] and is relatively easy to carry out. We call this the local DWIA approximation, and note that it is basically equivalent to the so-called factorized calculation first proposed by Laget [17]. Furthermore, if we replace the distorted pion and proton wave functions with plane waves, the matrix element takes the simple form

$$T^{\mathrm{PWIA}}(\alpha,\lambda,m_s) = \chi^\dagger_{m_s}\, t_{\gamma\pi}\, \Psi_\alpha(\mathbf{p}_i), \tag{11}$$

which is the production operator multiplied by the Fourier transform of the single particle bound wave function. This is called the plane wave impulse approximation (PWIA).

Now we discuss the procedure used to evaluate the six-dimensional integral in Eq. (10). In previous studies on (γ,π) [5–7], angular momentum recoupling was used to take advantage of the selection rules in the nuclear transitions from initial to final bound states. Since only certain transitions are allowed, the sums in angular momenta were very restricted. The situation for $(\gamma,\pi N)$ is quite different since the final nucleon is in the continuum. In principle, all partial waves are possible and it is no longer helpful to perform the angular momentum recoupling. Therefore we evaluate the six-dimensional integral by direct multiplication of the wave functions and production operator. The six-dimensional integral is split into a four-dimensional angular part and a two-dimensional "radial" part. The four-dimensional angular integral defined as

$$F(p',q',l_\pi,\kappa_p,\alpha,\lambda,m_s) = \sum_{\substack{m_l,m_l'\\ m_s^i\,m_s'}} \int d\Omega_{p'}\, d\Omega_{q'}\, \chi^\dagger_{m_s'}\, t_{\gamma\pi}(\lambda,\mathbf{k},\mathbf{p}_i,\mathbf{q}',\mathbf{p}')\, \chi_{m_s^i}\, \phi_\alpha(p_i) \times C^{l_p\ 1/2\ j_p}_{m_l'\ m_s\ m_p}\, C^{l_p\ 1/2\ j_p}_{m_l'\ m_s'\ m_p}\, C^{l\ 1/2\ j}_{m_l\ m_s^i\ m}\, Y^{l_p}_{m_l'}(\hat{\mathbf{p}})\, Y^{l_p *}_{m_l'}(\hat{\mathbf{p}}')\, P_{l_\pi}(\hat{\mathbf{q}}\cdot\hat{\mathbf{q}}')\, Y^{l}_{m_l}(\hat{\mathbf{p}}_i) \tag{12}$$

is evaluated first and stored in a large array. Then the "radial" part

$$T(\alpha,\lambda,m_s) = \sum_{l_\pi,\kappa_p} \int dp'\, dq'\, p'^2\, q'^2\, U_{\kappa_p}(p,p')\, U_{l_\pi}(q,q')\, F(p',q',l_\pi,\kappa_p,\alpha,\lambda,m_s) \tag{13}$$

is evaluated using appropriate prescriptions for handling the singularities in the momentum space wave functions. Gaussian integration methods are used in evaluating both integrals. For the case of starting with configuration wave functions, such a prescription is given in Ref. [6]. Finally, to achieve faster convergence of the partial waves, PWIA matrix elements are subtracted and added to the DWIA ones, resulting in the following expression:

$$T(\alpha,\lambda,m_s) = T^{\mathrm{PWIA}}(\alpha,\lambda,m_s) + \sum_{l_\pi,\kappa_p} \Bigg\{ \int dp'\, dq'\, p'^2\, q'^2 \left[U_{\kappa_p}(p,p')\, U_{l_\pi}(q,q') - \frac{(2l_\pi+1)}{4\pi}\, \frac{\delta(p-p')\,\delta(q-q')}{p^2\, q^2} \right] \times F(p',q',l_\pi,\kappa_p,\alpha,\lambda,m_s) \Bigg\}. \tag{14}$$

The numerical results have been checked using various criteria: (1) If the production operator is localized in Eq. (10), then the nonlocal DWIA result should reduce to the local DWIA result [see Eq. (6)]. (2) If in the local DWIA the radial distorted waves in Eqs. (8) and (9) are replaced by spherical Bessel functions, then the local DWIA should reduce to the PWIA. (3) To make sure that the optical potentials are implemented properly, if the strengths of the optical potentials are reduced to very small values, the DWIA results should also approach the PWIA results. All of the above have been confirmed numerically and in addition we have made the same checks when only the pion or nucleon had distorted waves included. Note that both the outgoing pion and nucleon usually have kinetic energies above 50 MeV so we have neglected the Coulomb distortions in the optical potentials.

By varying the number of integration points and partial waves, we find that for our kinematic region the following numbers are needed to get results good to 2%: 6 pion partial waves, 11 nucleon partial waves, 9 integration points in p' and q' with limits $p'_{\min} = 0.3p, p'_{\max} = 3p$ and $q'_{\min} = 0.3q$, $q'_{\max} = 3q$, 12 points in pion angular dimension, and 16 points in nucleon angular dimension. This amounts to using $9^2 \times 12^2 \times 16^2 = 2\,985\,984$ points to evaluate one integral for each index in pion and proton partial waves, photon polarization, proton spin, and m substates of the bound nucleon. For the $p_{3/2}$ shell there are about $6 \times 23 \times 2 \times 2 \times 4 = 2208$ such integrals to be evaluated to get one point in a plot. These extensive numerical integrations and summations can only be accomplished with the help of supercomputers.

IV. RESULTS AND DISCUSSIONS

In this section we first compare our calculations to the existing data for $(\gamma, \pi N)$, then make some suggestions for future experiments.

A. Comparison to Tomsk data

Figure 2 shows the comparison between one experiment done at the Tomsk synchrotron [13] and the PWIA, local DWIA and nonlocal DWIA calculations for the case of $(\pi^- p)$ production from the neutrons in the $1s_{1/2}$ and $1p_{3/2}$ shells of ^{12}C. The triple coincidence cross sections are plotted as a function of the proton energy for fixed photon energy and backward (120°) pion angle and forward proton angle (20°). The pions and protons were detected in coincidence in the production plane by two spectrometers sitting on opposite sides of the photon beam. Under this kinematics, the pion energy T_π, the momentum transfer Q, and the invariant mass W all change with T_p. For example, in the case of the $1s$ shell, in the range of T_p from 50 to 190 MeV, T_π decreases from 148 to 8 MeV; Q starts at 241 MeV/c, drops down to 10 MeV/c and then increases again to 253 MeV/c; and W ranges from 1260 to 1130 MeV. The kinematics for the $1p$ shell are similar, only differing because of the different binding energy. The shapes of the curves follow the momentum

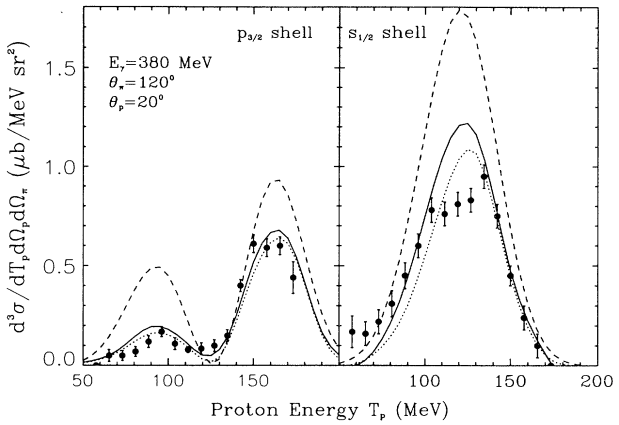

FIG. 2. Proton energy dependence of the triple coincidence cross section from $p_{3/2}$ and $s_{1/2}$ shell neutrons in $^{12}C(\gamma, \pi^- p)^{11}C$ for fixed E_γ, θ_π, and θ_p. Theoretical curves are calculated in PWIA (dashed line), local DWIA (dotted line), and nonlocal DWIA (solid line). Data are taken from Ref. [13].

distribution of the bound neutron, namely, the minimum in Q corresponds to the minimum of the cross section in the $1p$ shell case and the maximum in the $1s$ shell case. Thus, these kinematics can be used to obtain information on the neutron wave functions, which was one of the purposes of the experiment. The DWIA calculations give a good description of the cross section measured in terms of both shape and magnitude, while the PWIA results overestimate the data considerably. The distortion effects from final-state interactions reduce the cross section and are important in explaining the data. The nonlocal DWIA computations tend to enhance the local DWIA results and here improve the agreement between the theory and the experiment. Note that we have used s-shell and p-shell spectroscopic factors of $S_{s_{1/2}} = 1.3$ and $S_{p_{3/2}} = 2.6$. In Ref. [13], a factorized DWIA with an eikonal approximation for the outgoing pion and nucleon was used to analyze the data; however, we could not tell whether or not a spectroscopic factor was used in the analysis.

Figure 3 shows the comparison with another experiment on $^{12}C(\gamma, \pi^- p)^{11}C$ from Tomsk [14]. The combined s- and p-shell contributions to the triple cross section are shown as a function of the proton energy for four different pion energies 44.3, 65.5, 97.7, and 118.4 MeV. The pion angle is held at 120° and proton angle at 40° on the other side of the photon beam. In this kinematic setup, the photon energy E_γ, the invariant mass W, and the momentum transfer Q are not fixed. Examining the $1p$ shell separately, both E_γ and W increase with T_p, while Q has minima located at T_p approximately equal to 40, 50, 75, and 90 MeV for each of the four pion energies. The values of these $Q_{\min}$ are 116, 130, 155, and 173 MeV/c, respectively. The data are somewhat higher than the theoretical curves while the shapes are reasonably reproduced. Again including nonlocal effects improves the agreement between our calculation and the data. More

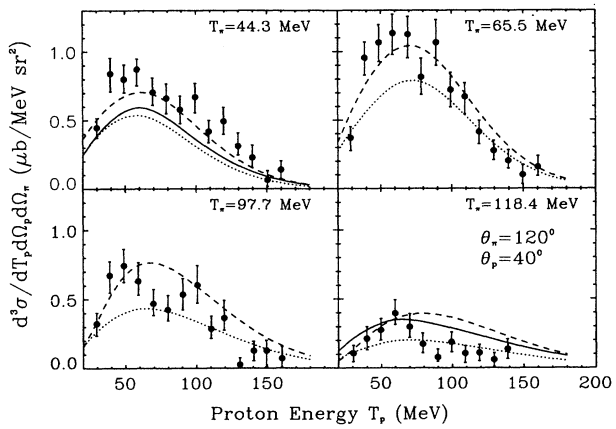

FIG. 3. Proton energy distributions of the differential cross section from combined s and p shell neutrons in ^{12}C at fixed θ_π and θ_p are shown at four different pion energies. Theoretical curves are calculated in PWIA (dashed line), local DWIA (dotted line), and nonlocal DWIA (solid line). Data are taken from Ref. [14].

detailed comparisons are not permitted because of the relatively large error bars and the scatter in the data, especially in the $T_\pi = 97.7$ MeV and $T_\pi = 118.4$ MeV cases. The photon energy in this experiment was not very well defined, with E_γ ranging from 317 to 363 MeV.

B. Comparison to Bates data

In Fig. 4 the PWIA and local DWIA calculations are compared to the experimental data from Bates [15] for the reaction $^{16}\mathrm{O}(\gamma,\pi^- p)^{15}\mathrm{O}$. The experimental setup allows out-of-plane measurements. Data were taken at two pion angles, 64° and 120°, while a vertical array of proton detectors were positioned at proton angles 40° and 20° corresponding to free two-body kinematics with the momentum transfer being zero. The out-of-plane proton angle goes from 33° below the scattering plane to 33° above the scattering plane corresponding to the momentum transfer Q from about 190 MeV/c to 0 then to 190 MeV/c again. The forward pion case corresponds to higher pion energy (145 MeV) and lower proton energy (58 MeV), while the backward pion setup is just the opposite: lower pion energy (89 MeV), higher proton energy (114 MeV). The invariant mass does not change much, from 1225 to 1223 MeV, which stays in the Δ region.

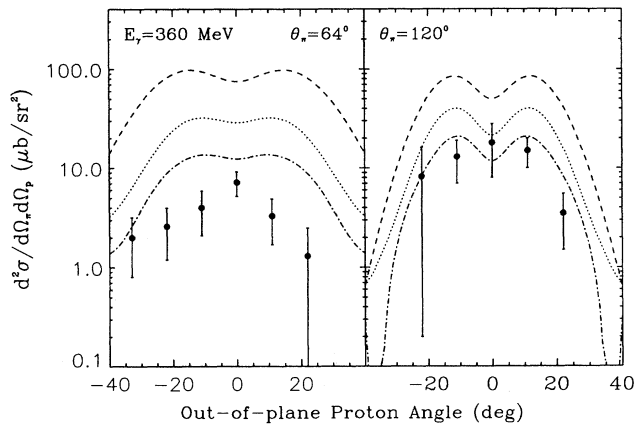

FIG. 4. Out-of-plane proton angular dependence of the integrated coincidence cross section from combined $p_{3/2}$ and $p_{1/2}$ shell neutrons in $^{16}\mathrm{O}(\gamma,\pi^- p)^{15}\mathrm{O}$ for fixed photon energy and two pion angles. Theoretical curves are calculated in PWIA (dashed line) and local DWIA (dotted line). The dash-dotted curve is calculated in local DWIA with the Δ mass reduced by 5%. Data are taken from Ref. [15].

Unfortunately, due to low counting rates, the data were integrated over a wide range of pion energies:

$$\frac{d^2\sigma}{d\Omega_\pi\, d\Omega_p} = \int_{T_\pi^{\min}}^{T_\pi^{\max}} dT_\pi \left(\frac{d^3\sigma}{dT_\pi\, d\Omega_\pi\, d\Omega_p} \right), \qquad (15)$$

and therefore are not truly exclusive. This introduces a great deal of uncertainty in the data because each data point now contains a wide spectrum of momentum transfer Q. In making our comparisons we have tried to carry out the same integrations as done experimentally. Our calculations retain a slight minimum at $Q = 0$ (in the scattering plane) while the experimental data do not. As expected, distortion reduces the cross section by about a factor of 2–4, but does little to change the shape and location of the peaks. Our calculations include contributions from the $p_{3/2}$ and $p_{1/2}$ shells and we use a combined spectroscopic factor of $S_{1p} = 3.6$. The local DWIA calculations are in reasonable agreement with the data for backward pions, but exceed the data for forward pions by about a factor of 3. This discrepancy at forward pion angles—which was already pointed out in Refs. [15] and [16]—is reminiscent of similar results obtained in $(\pi,\pi' N)$ measurements [2]. Kinematically, the forward pion angle region corresponds to higher pion kinetic energies. This may hint at an inadequate description of the pion final-state interaction. However, the optical potential employed does successfully describe the Tomsk data for the same pion energies. Furthermore, our local DWIA results are in agreement with the calculations of Ref. [15] that has used an older parametrization of the pion optical potential but found that using different parametrizations modified the calculated cross sections by only 20%. Another difference between forward and backward pion angles has its origins in the structure of the elementary photoproduction operator. The Δ-resonance contribution dominates forward pion angles while the nonresonant Born terms are more important at backward angles. This applies to the elementary process as well as the reaction on the nucleus. As a matter of fact, we found that the discrepancy at the forward pion angle is largely removed by reducing the Δ mass by about 5% in our local DWIA calculation (see the dash-dotted curve in Fig. 4). Moreover, the reduction in the cross sections is differential for forward and backward pion angles; namely, it reduces the cross section more at the forward pion angle than at the backward pion angle. This strongly suggests that Δ medium effects may be responsible for the ob-

served discrepancy. This reduction of the Δ mass in the medium is clearly speculative and more dynamic studies coupled with better data are needed before any conclusion can be reached.

We have not carried out our nonlocal DWIA calculation for the Bates experiment since integrating over the pion energy requires too much computer time. Furthermore we find in our local DWIA calculation that our results are quite sensitive to the exact range of pion energies included. Both the magnitude and the shape vary with different limits of pion energies. In Fig. 5 we investigate nonlocal effects for the exclusive reaction from the $p_{1/2}$ shell in ^{16}O using the Bates kinematics with the pion energy fixed at its in-plane zero-momentum-transfer values. For the forward pion case we find a large enhancement in the cross section due to nonlocal effects, while at the backward pion angle the nonlocal enhancement is much smaller. Previous calculations of $A(\gamma,\pi)B$ reactions to specified nuclear states [5, 6, 11] already found that nonlocalities are more significant at higher pion energies. Consequently, the nonlocal calculation of the Bates integrated experiment will probably deviate even more for the forward pion case.

We want to point out here that the kinematics for the Tomsk experiments and the Bates experiment are not the same. In the Tomsk experiments, energy dependence of the reaction is studied for the backward pion angle (120°) only, while in the Bates experiment angular dependence of the reaction is investigated for both forward and backward pion angles. Thus the two data sets do not check each other. The discrepancy between theory and data for forward pions stands on its own and deserves further attention from both theory and experiment.

C. Suggestions for future experiments

In this section we give some guidance for planning future experiments of the reaction. In order to get a broader prospective, two three-dimensional plots, calculated in PWIA, of cross section and photon asymmetry for fixed pion and momentum transfer angles are shown in Figs. 6 and 7. The resonance peak is clearly seen in the cross section plot. We examined the Born and Δ contributions to the cross section separately and found that there is large destructive interference for $E_\gamma = 400$ MeV to 600 MeV. As shown in Fig. 7, the photon asymmetries are predicted to be large and positive at higher photon energies for lower values of Q.

In the following we present cross section and photon asymmetry results using the "fixed" in-plane kinematics that we proposed in Sec. III. All of our results used a ^{12}C target but other nuclei could also be studied.

In Fig. 8 we show the pion angular dependence of the cross section and the photon asymmetry calculated in PWIA, local DWIA, and full nonlocal DWIA for photon energy $E_\gamma = 360$ MeV, momentum transfer Q=150 MeV/c and pion energy $T_\pi = 100$ MeV. With these values, the pion angle can only range from 60° to 180°. More forward pion angles can be explored by increasing Q and T_π or decreasing E_γ. However, we should point out that higher Q will cause the counting rate to decrease; higher T_π will result in more uncertainties in pion distorted waves; lower E_γ will decrease the effects we are interested in because we are going away from the Δ region. The proton energy for these kinematics is $E_p = 103$ MeV and the proton angle θ_p ranges from about 41° to 13°. The invariant mass W goes from 1197 to 1253 MeV. Nonlocal effects enhance the local DWIA cross sections. The striking feature is that the photon asymmetry is insensitive both to distortions and to nonlocal effects. This removes the uncertainties that may obscure the information from the production process. Thus, PWIA is a good approximation for calculating the photon asymmetry in this reaction. Further, the photon asymmetry is a relatively "clean" observable and therefore should be considered in planning future experiments.

In Figs. 9 and 10, individual contributions from Born

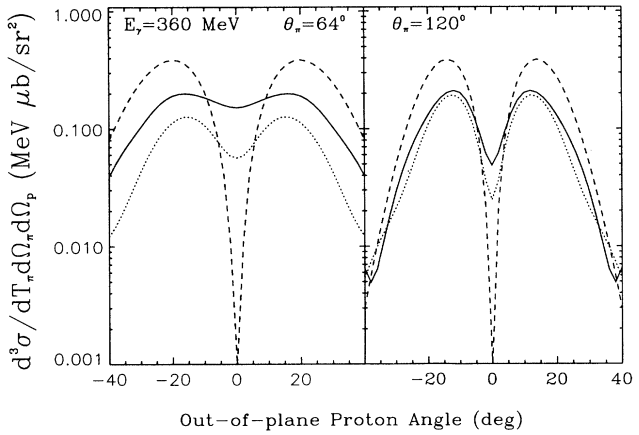

FIG. 5. Out-of-plane proton angular dependence of the true coincidence cross section from $p_{1/2}$ shell neutrons in ^{16}O$(\gamma,\pi^-p)^{15}$O for fixed photon energy and two pion angles. Theoretical curves are calculated in PWIA (dashed line), local DWIA (dotted line), and nonlocal DWIA (solid line).

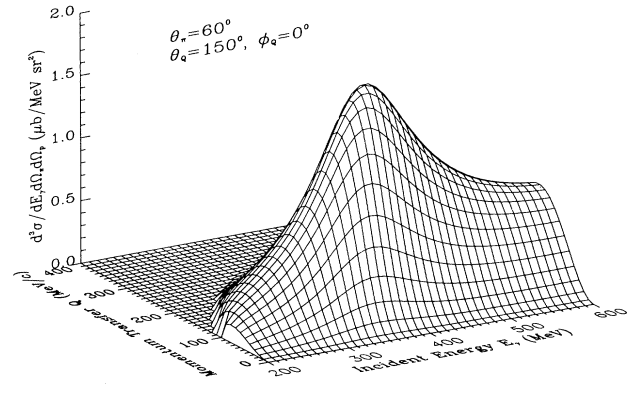

FIG. 6. The Δ resonance peak from $p_{3/2}$ shell neutrons in ^{12}C$(\gamma,\pi^-p)^{11}$C is displayed by the three-dimensional plot of the cross section as a function of the photon energy and the momentum transfer at fixed pion angle and fixed direction of the momentum transfer. It is calculated in PWIA.

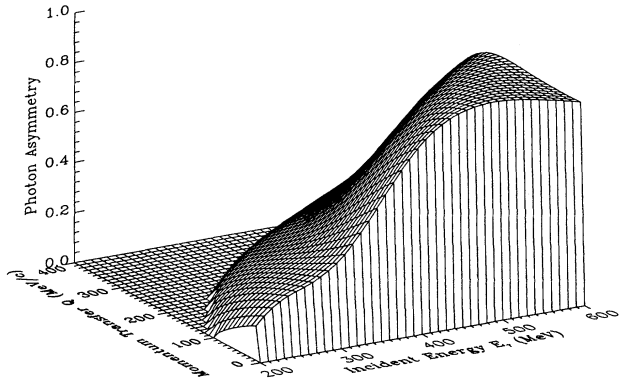

FIG. 7. Same as in Fig. 6, but for the photon asymmetry.

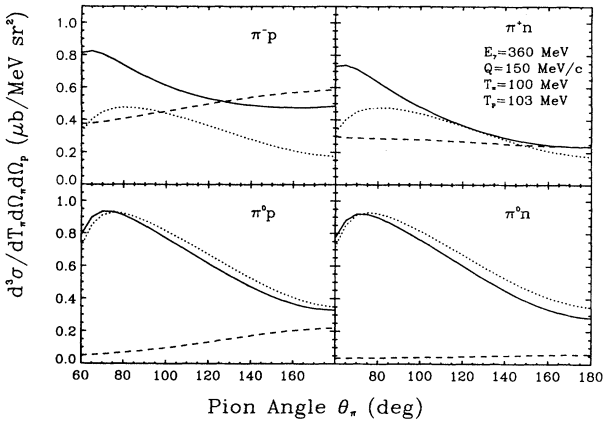

FIG. 9. The individual contributions to the cross sections from Born and Δ terms in the production operator are given for all four channels of pion photoproduction. The calculation is done in PWIA. The dashed curves are from Born terms only, dotted curves are from Δ terms only, and the solid curves are from the full operator. The same kinematics and target as in Fig. 8 are used.

and Δ terms are given for all four channels of pion photoproduction. For the cross section, the Δ terms are larger than the Born terms at forward pion angles. In the cases of π^0 production, the Δ terms are almost completely dominant as expected. For the photon asymmetry, the Δ contributions are always larger than the Born contributions and thus most of the photon asymmetry is from the Δ resonance. Should an experiment find deviations of the photon asymmetry from the simple PWIA predictions, this would indicate medium modifications of the Δ propagator.

Since no Δ-hole calculation is yet available for this exclusive reaction, we are interested in testing the sensitivity of the observables to the parameters in the model. In the model of Blomqvist and Laget [21, 22], the mass M_Δ, width Γ_Δ, and coupling constant G_3 of the Δ were treated as free parameters and fitted to the elementary pion photoproduction data. In a consistent many-body calculation these parameters would be modified by the surrounding nuclear medium. However, lacking such a calculation and recalling that a reduction of M_Δ by 5% improved the agreement with the Bates data, we are at the present time merely interested in obtaining a qualitative understanding of the sensitivities in our calculation. In Figs. 11 and 12 we show the effects of increasing and decreasing M_Δ, Γ_Δ, and G_3 by 3%. Obviously there is a great sensitivity to small percentage variations in the Δ mass (amounting to about 40 MeV) both in the cross section and in the photon asymmetry compared to very

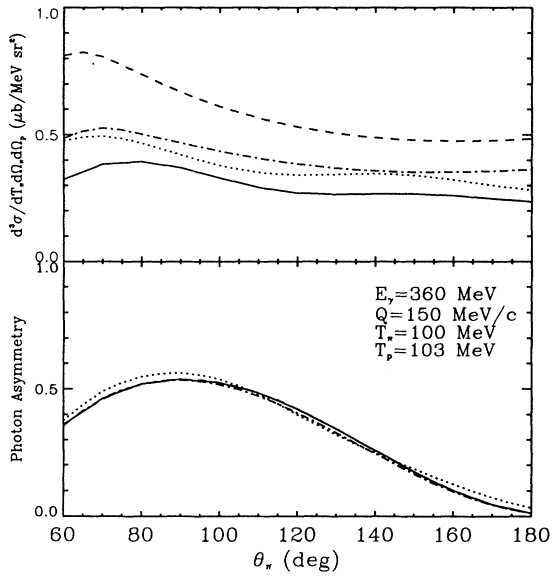

FIG. 8. The cross section and the photon asymmetry are shown in the "fixed" kinematics specified in the text for $p_{3/2}$ neutrons in $^{12}C(\gamma,\pi^- p)^{11}C$. Curves are calculated in PWIA (dashed line), local DWIA (solid line), and nonlocal DWIA with pion distortion only (dotted line) and proton distortion only (dot-dashed line).

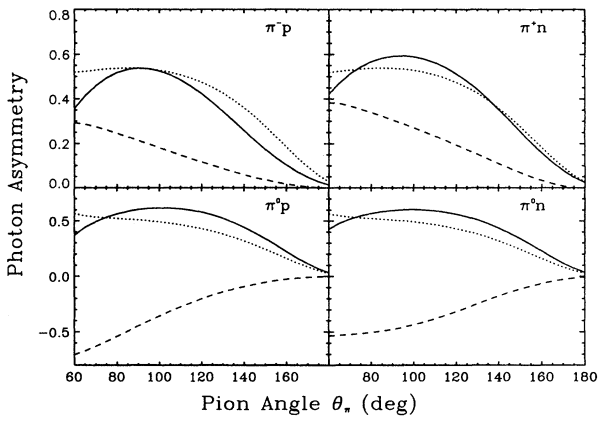

FIG. 10. Same as Fig. 9, but for the photon asymmetry.

little sensitivity to the other parameters. This "effective" Δ mass is closely related to the Δ-nucleus interaction in the Δ-hole theory.

In Fig. 13 we show the Δ mass effects on cross section and photon asymmetry for pion energy $T_\pi = 130$ MeV. Again the drop in cross section is differential, namely, more at forward pion angles than at backward angles. The change in the shape of the photon asymmetry is a clear signal of possible medium modification. Note that at the forward pion angle $\theta_\pi = 64°$, the kinematic conditions here are very similar to those in the Bates experiment; therefore it can be used to check the anomaly revealed by the Bates experiment.

It is well known that the Δ with $J^\pi = \frac{3}{2}^+$ is basically a quark spin-flip excitation of the nucleon which corresponds to a magnetic dipole ($M1$) if the electromagnetic interaction is used as the excitation mechanism. However, the presence of possible transverse ($E2$) and longitudinal ($C2$) quadrupole amplitudes has generated a lot of interest since they would be an indication of a tensor component in the quark-quark interaction which leads to a small d state component and results in the spatial asymmetry of the Δ wave function (referred to as the

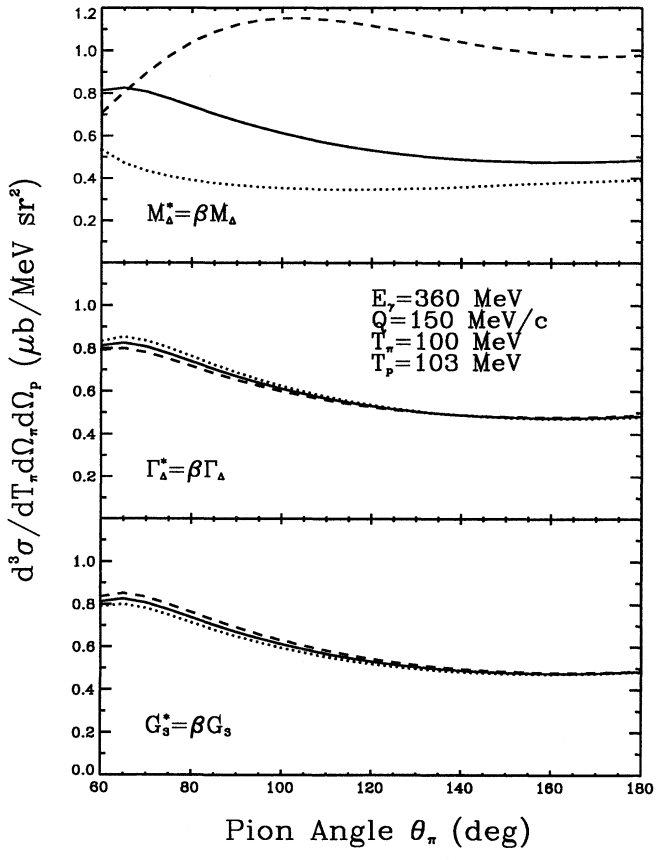

FIG. 11. Sensitivity of the cross section to the parameters in the model. Here M_Δ, Γ_Δ, and G_3 are the mass, width, and coupling constant of the Δ, respectively. The dashed line is for $\beta = 1.03$, dotted line for $\beta = 0.97$, and solid line for $\beta = 1.00$. The calculation is done in PWIA.

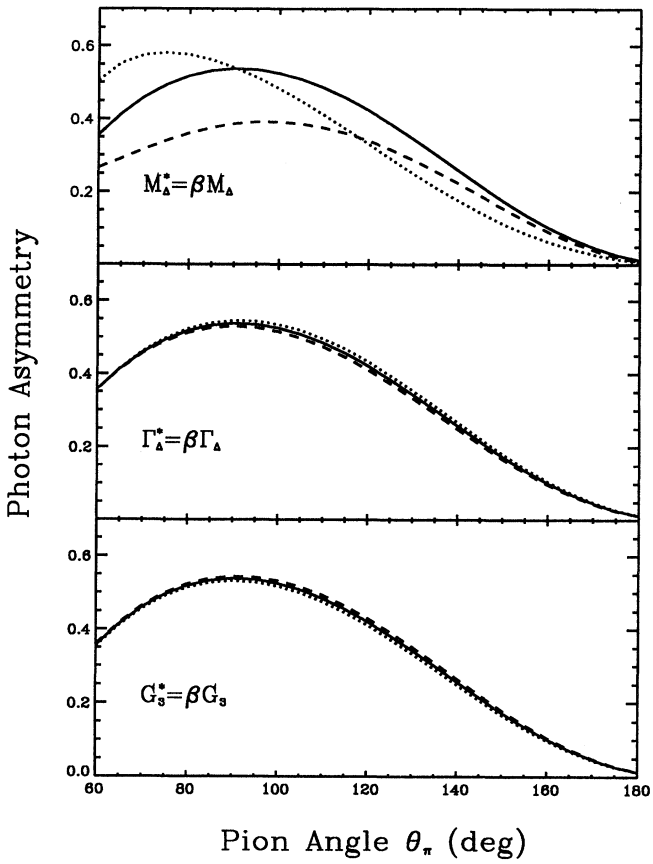

FIG. 12. Same as Fig. 11, but for the photon asymmetry.

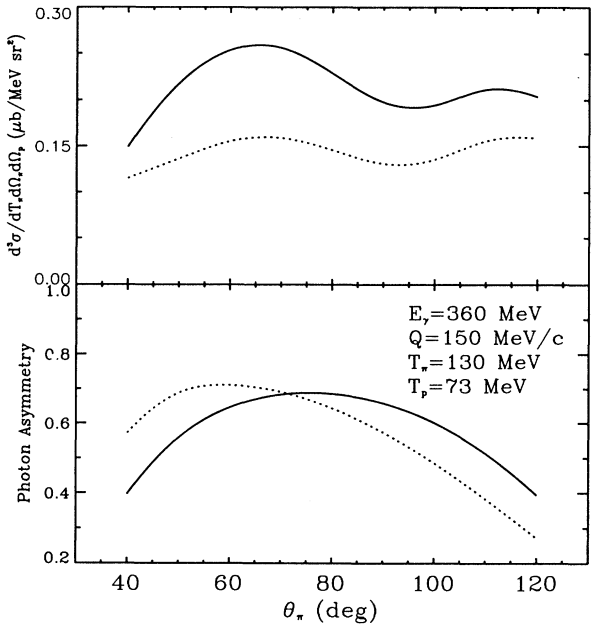

FIG. 13. Effects on the cross section and photon asymmetry by reducing the Δ mass at pion energy $T_\pi = 130$ MeV. The solid line is the full curve without the mass change; the dotted line is with the Δ mass reduced by 3%. The calculation is carried out in local DWIA.

deformation of the Δ). The N-Δ $E2$ component can only be extracted with aid of a model and the $E2/M1$ ratio ranges from 0 to -5% depending on the theoretical approach invovled. The Particle Data Tables give a value [23]: $E2/M1 = -1.3 \pm 0.5\%$ which does not yet reflect the model dependency present in the multipole analysis. One might therefore speculate that the $E2$ transition which arises from a small admixture into the wave function is more susceptible to nuclear modifications than $M1$ which merely involves a spin flip on s-state quarks. We are thus interested if such modifications could be detected using the $(\gamma, \pi N)$ reaction on complex nuclei. It has been shown in a recent calculation for $^3\mathrm{He}(\gamma,\pi^+)^3\mathrm{H}$ [29] that the photon asymmetry is very sensitive to the $E2$ multipole. In Fig. 14 the sensitivity in this reaction to the $E2$ component is shown for three cases. We modify the $E2$ amplitude by changing the parameter α [see Eq. (A14)] which is a measure of the relative strength and phase between the $M1$ and the $E2$ transitions. Laget's value for α is 0.8, and we show the resulting curves for $\alpha = 0$ and $\alpha = -0.8$. While such a change is clearly arbitrary at this point, it reveals the sensitivity in the cross section to the $E2$ amplitude at backward pion angle and in the photon asymmetry around 90°.

Finally, we look at the possibility of using this reaction $(\gamma, \pi^- p)$ to investigate the neutron wave functions which are usually difficult to study by other means. To avoid uncertainties, one wants to stay away from the Δ. Thus we have chosen $E_\gamma = 260$ MeV to illustrate this point. In Fig. 15 the cross section is plotted as a function of the momentum transfer for three different values of b (the harmonic oscillator range parameter). The sensitivities displayed for $p_{3/2}$ and $s_{1/2}$ orbitals can be used to obtain information on neutron wave functions.

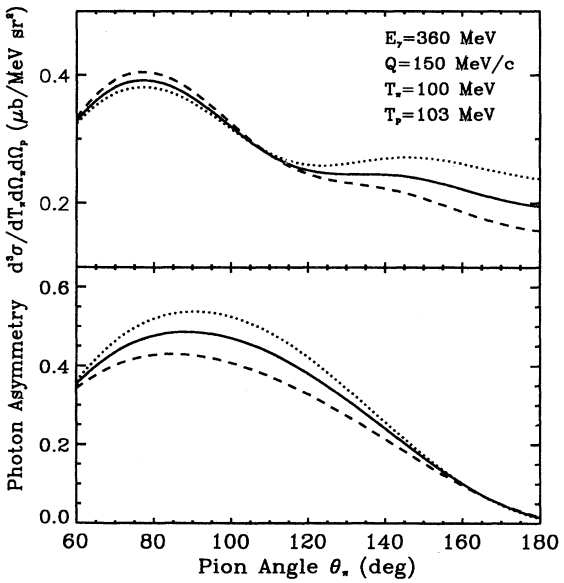

FIG. 14. Sensitivity to different $E2$ multipole components. The quantity α, defined in Ref. [22], measures the relative strength between $M1$ and $E2$ transitions of the Δ. The dashed line is for $\alpha = -0.8$, dotted line for $\alpha = 0.8$, and solid line for $\alpha = 0$. The calculation is carried out using local DWIA.

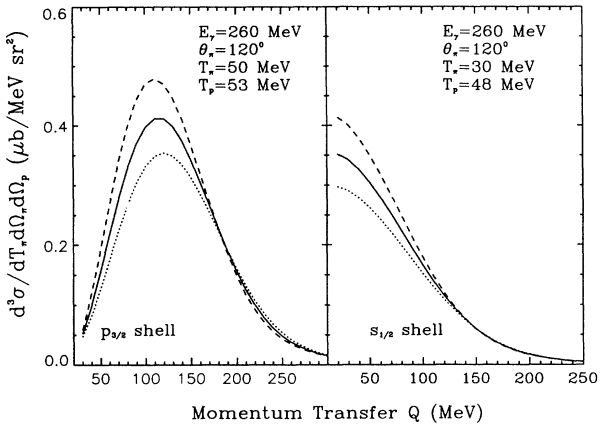

FIG. 15. Cross sections as a function of the momentum transfer Q are plotted for $p_{3/2}$ and $s_{1/2}$ shell neutrons in $^{12}\mathrm{C}(\gamma,\pi^- p)^{11}\mathrm{C}$ to show the sensitivity to the bound neutron wave functions characterized by harmonic oscillator range parameter b. The dashed line is for $b = 1.82$ fm, dotted line for $b = 1.64$ fm, and solid line for $b = 1.73$ fm. The calculation is carried out using local DWIA.

V. CONCLUSIONS

The exclusive $A(\gamma, \pi N)B$ reaction offers an ideal laboratory for studying the Δ resonance in the nuclear medium. It allows for more direct access to the Δ than the reaction $A(\gamma, \pi)B$ since the final nucleon is no longer bound and the sensitivity to the nuclear structure of the target is thereby greatly reduced. The only information required for the target is the single particle bound wave function and the spectroscopic factor, which is only an overall factor in the cross section. Kinematically, the reaction provides a great deal of flexibility since the target can take up a wide range of momentum transfer and for finite nuclei, little energy. We have proposed a kinematic arrangement that can best expose the information from the production vertex by fixing the lengths of each momentum vector in the overall momentum conservation.

We have successfully established the first full nonlocal DWIA calculation for the exclusive reaction $A(\gamma, \pi N)B$ in the Δ region. All previous computations for this process [13–16] were performed in a factorized, local approximation developed by Laget [17]. Comparison with the existing data suggest that it contains the correct basic ingredients. More experiments are needed to fully investigate this very promising reaction and, in fact, such efforts are already in progress [16, 20].

The photon asymmetry is a very good observable to complement the cross section measurements. It comes mainly from the Δ resonance, is free from normalization problems, is predicted to be large, and is relatively insensitive to the distortions and nonlocal effects. It should definitely be pursued at accelerators with the capability

of polarized photon beams. As far as the local DWIA calculation is concerned, the distortions from final-state interactions always attenuate the PWIA cross sections. Although distortion plays an important role in getting the correct magnitudes, it does little to change the shape of the curves. Nonlocal effects always enhance the local DWIA cross sections and in some cases they are quite significant. In general, quantitative comparison of theory and experiment requires a nonlocal calculation. We find a great sensitivity of the calculated cross sections and photon asymmetries to the Δ mass. Within our local DWIA analysis, it appears to be able to explain the disagreement between the Bates data and theoretical predictions at the forward pion angle if the Δ mass is reduced by about 5%. A dynamical model such as the Δ-hole model is needed in order to resolve the discrepancy by properly including the medium modifications.

Finally, we intend to extend the calculation to the virtual photon case, namely, pion electroproduction from complex nuclei $A(e,e'\pi N)B$ in order to study the longitudinal response of the production process in the nuclear medium. Such an effort is underway. Beyond that, one can go to higher energies to study other meson production reactions, such as kaon production and eta production. Our formalism can also be applied to study the time reversal reaction $A(\pi,\gamma N)B$, e.g., radiative pion capture by nuclei.

ACKNOWLEDGMENTS

We would like to thank the Ohio Supercomputer Center for time on the Cray Y-MP. This research was supported in part by the U.S. DOE under Grant No. FG02-87ER40370 and DE-FG05-86-ER40270, and a NATO Collaborative Research Grant.

APPENDIX: BLOMQVIST-LAGET PION PHOTOPRODUCTION OPERATOR

For completeness, we give the full operator for both charged and neutral pion photoproductions. The operator is written as $t_{\gamma\pi} = \boldsymbol{\epsilon}_\lambda \cdot \mathbf{J}$ where $\boldsymbol{\epsilon}_\lambda$ is the photon polarization vector and $\mathbf{J}$ is the pion photoproduction current. We decompose the operator into spin 0 and spin 1 terms by writing

$$t_{\gamma\pi}(\lambda, \mathbf{k}, \mathbf{p}_i, \mathbf{q}, \mathbf{p}) = L + i\,\boldsymbol{\sigma} \cdot \mathbf{K}. \tag{A1}$$

The non-spin-flip term L and the spin-flip term $\mathbf{K}$ each consist of a coherent sum of the Born and Δ resonance terms:

$$L = L_{\rm Born} + L_\Delta, \tag{A2}$$

$$\mathbf{K} = \mathbf{K}_{\rm Born} + \mathbf{K}_\Delta. \tag{A3}$$

The Born terms in PV coupling for various production channels are given by the following. For $\gamma + p \to \pi^+ + n$:

$$L_{\rm Born} = \frac{\sqrt{2}\,e g_0}{2m}\left[\frac{\mu_p}{2E_a(P_a^0 - E_a)} + \frac{\mu_n}{2E_b(P_b^0 - E_b)}\right] \mathbf{q}\cdot(\mathbf{k}\times\boldsymbol{\epsilon}_\lambda), \tag{A4}$$

$$\mathbf{K}_{\rm Born} = \frac{\sqrt{2}\,e g_0}{2m}\left\{\left[-1 + \frac{mE_\pi}{E_a(P_a^0 + E_a)}\right]\boldsymbol{\epsilon}_\lambda + \frac{\boldsymbol{\epsilon}_\lambda\cdot\mathbf{q}\,(\mathbf{k}-\mathbf{q})}{E_\gamma E_\pi - \mathbf{k}\cdot\mathbf{q}} - \frac{\boldsymbol{\epsilon}_\lambda\cdot\mathbf{p}_i\,\mathbf{q}}{E_a(P_a^0 - E_a)} + \left[\frac{\mu_p}{2E_a(P_a^0 - E_a)} - \frac{\mu_n}{2E_b(P_b^0 - E_b)}\right]\mathbf{q}\times(\mathbf{k}\times\boldsymbol{\epsilon}_\lambda)\right\}. \tag{A5}$$

For $\gamma + n \to \pi^- + p$:

$$L_{\rm Born} = \frac{\sqrt{2}\,e g_0}{2m}\left[\frac{\mu_n}{2E_a(P_a^0 - E_a)} + \frac{\mu_p}{2E_b(P_b^0 - E_b)}\right] \mathbf{q}\cdot(\mathbf{k}\times\boldsymbol{\epsilon}_\lambda), \tag{A6}$$

$$\mathbf{K}_{\rm Born} = \frac{\sqrt{2}\,e g_0}{2m}\left\{\left[1 + \frac{mE_\pi}{E_b(P_b^0 + E_b)}\right]\boldsymbol{\epsilon}_\lambda - \frac{\boldsymbol{\epsilon}_\lambda\cdot\mathbf{q}\,(\mathbf{k}-\mathbf{q})}{E_\gamma E_\pi - \mathbf{k}\cdot\mathbf{q}} - \frac{\boldsymbol{\epsilon}_\lambda\cdot\mathbf{p}\,\mathbf{q}}{E_b(P_b^0 - E_b)} + \left[\frac{\mu_n}{2E_a(P_a^0 - E_a)} - \frac{\mu_p}{2E_b(P_b^0 - E_b)}\right]\mathbf{q}\times(\mathbf{k}\times\boldsymbol{\epsilon}_\lambda)\right\}. \tag{A7}$$

For $\gamma + p \to \pi^0 + p$:

$$L_{\rm Born} = \frac{e g_0}{2m}\left[\frac{\mu_p}{2E_a(P_a^0 - E_a)} + \frac{\mu_p}{2E_b(P_b^0 - E_b)}\right]\left(\mathbf{q} - \frac{E_\pi}{2m}(2\mathbf{p}_i - \mathbf{q})\right)\cdot(\mathbf{k}\times\boldsymbol{\epsilon}_\lambda), \tag{A8}$$

$$\mathbf{K}_{\rm Born} = \frac{eg_0}{2m}\left\{\left[\frac{\mu_p}{2E_a(P_a^0-E_a)} - \frac{\mu_p}{2E_b(P_b^0-E_b)}\right]\left(\mathbf{q}-\frac{E_\pi}{2m}(2\mathbf{p}_i-\mathbf{q})\right)\times(\mathbf{k}\times\boldsymbol{\epsilon}_\lambda)\right.$$
$$-\frac{\boldsymbol{\epsilon}_\lambda\cdot\mathbf{p}_i}{E_a(P_a^0-E_a)}\left[\mathbf{q}-\frac{E_\pi}{2m}(\mathbf{q}+2\mathbf{p})\right] - \frac{\boldsymbol{\epsilon}_\lambda\cdot\mathbf{p}}{E_b(P_b^0-E_b)}\left[\mathbf{q}-\frac{E_\pi}{2m}(2\mathbf{p}_i-\mathbf{q})\right]$$
$$+\boldsymbol{\epsilon}_\lambda\left[\frac{m}{E_a(P_a^0+E_a)}\left(E_\pi-\frac{(2\mathbf{p}+\mathbf{q})\cdot\mathbf{q}}{2m}\right)\left(1-\frac{E_\pi}{2m}\kappa_p\right)\right]$$
$$\left.+\boldsymbol{\epsilon}_\lambda\left[\frac{m}{E_b(P_b^0+E_b)}\left(E_\pi-\frac{(2\mathbf{p}_i-\mathbf{q})\cdot\mathbf{q}}{2m}\right)\left(1+\frac{E_\pi}{2m}\kappa_p\right)\right]\right\}. \tag{A9}$$

For $\gamma + n \to \pi^0 + n$:

$$L_{\rm Born} = \frac{eg_0}{2m}\left[\frac{\mu_n}{2E_a(P_a^0-E_a)} + \frac{\mu_n}{2E_b(P_b^0-E_b)}\right]\left(\mathbf{q}-\frac{E_\pi}{2m}(2\mathbf{p}_i-\mathbf{q})\right)\cdot(\mathbf{k}\times\boldsymbol{\epsilon}_\lambda), \tag{A10}$$

$$\mathbf{K}_{\rm Born} = \frac{eg_0}{2m}\left\{\left[\frac{\mu_n}{2E_a(P_a^0-E_a)} - \frac{\mu_n}{2E_b(P_b^0-E_b)}\right]\left(\mathbf{q}-\frac{E_\pi}{2m}(2\mathbf{p}_i-\mathbf{q})\right)\times(\mathbf{k}\times\boldsymbol{\epsilon}_\lambda)\right.$$
$$-\boldsymbol{\epsilon}_\lambda\left[\frac{m}{E_a(P_a^0+E_a)}\left(E_\pi-\frac{(2\mathbf{p}+\mathbf{q})\cdot\mathbf{q}}{2m}\right)\left(\frac{E_\pi}{2m}\kappa_n\right)\right]$$
$$\left.+\boldsymbol{\epsilon}_\lambda\left[\frac{m}{E_b(P_b^0+E_b)}\left(E_\pi-\frac{(2\mathbf{p}_i-\mathbf{q})\cdot\mathbf{q}}{2m}\right)\left(\frac{E_\pi}{2m}\kappa_n\right)\right]\right\}. \tag{A11}$$

The photon, incoming nucleon, pion, and outgoing nucleon four-momenta are $k^\mu = (E_\gamma, \mathbf{k})$, $p_i^\mu = (E_{p_i}, \mathbf{p}_i)$, $q^\mu = (E_\pi, \mathbf{q})$, and $p^\mu = (E_N, \mathbf{p})$, respectively. They can be in any reference frame. The polarization vector of the photon is $\boldsymbol{\epsilon}_\lambda$ and m is the nucleon mass. The four-momenta in the s and u channels are $P_a^\mu = k^\mu + p_i^\mu$ and $P_b^\mu = p_i^\mu - q^\mu = p^\mu - k^\mu$ and $E_{a,b} = (|\mathbf{P}_{a,b}|^2 + m^2)^{1/2}$. The magnetic moments of the nucleons are $\mu_p = 1 + \kappa_p = 2.79$ and $\mu_n = \kappa_n = -1.91$ and for the $\pi - N$ coupling constant we use $g_0^2/4\pi = 14$.

In the π^0 channels, the following ω-exchange term should be added coherently to L:

$$L_\omega = \frac{1}{m_\pi}\frac{g_{\omega_1} g_{\gamma\pi\omega}}{(q^\mu - k^\mu)^2 - m_\omega^2}\,\mathbf{q}\cdot(\mathbf{k}\times\boldsymbol{\epsilon}_\lambda), \tag{A12}$$

where $m_\omega = 750$ MeV, $g_{\omega_1} = 10$, and $g_{\gamma\pi\omega} = 0.374$.

The Δ resonance terms with both $M1$ and $E2$ transitions are given by

$$L_\Delta = -\frac{eC_\pi C_\gamma G_1 G_3\, e^{i\phi_M}}{P_a^2 - M_\Delta^2 + i\,\Gamma_\Delta M_\Delta}\frac{2}{3}\left[\frac{E_\pi}{m}\mathbf{p}_i\cdot(\mathbf{k}\times\boldsymbol{\epsilon}_\lambda) + \frac{M_\Delta - m}{m}\mathbf{q}\cdot(\mathbf{p}_i\times\boldsymbol{\epsilon}_\lambda) - \mathbf{q}\cdot(\mathbf{k}\times\boldsymbol{\epsilon}_\lambda)\right], \tag{A13}$$

$$\mathbf{K}_\Delta = -\frac{eC_\pi C_\gamma G_1 G_3}{P_a^2 - M_\Delta^2 + i\,\Gamma_\Delta M_\Delta}\left\{\left(\boldsymbol{\epsilon}_\lambda\cdot\mathbf{q} - \frac{E_\pi}{M_\Delta}\boldsymbol{\epsilon}_\lambda\cdot\mathbf{p}_i\right)\left(\mathbf{k} - \frac{M_\Delta - m}{m}\mathbf{p}_i\right)\left(\frac{1}{3}e^{i\phi_M} + \frac{2M_\Delta\,\omega\,\alpha}{(3M_\Delta + m)(M_\Delta + m)}e^{i\phi_E}\right)\right.$$
$$+\left[-\mathbf{k}\cdot\mathbf{q} + \frac{E_\pi}{M_\Delta}(E_\gamma^2 + \mathbf{k}\cdot\mathbf{p}_i) + \frac{M_\Delta - m}{m}\left(\mathbf{p}_i\cdot\mathbf{q} - \frac{E_\pi}{M_\Delta}(|\mathbf{p}_i|^2 + \mathbf{k}\cdot\mathbf{p}_i)\right)\right]\boldsymbol{\epsilon}_\lambda$$
$$\left.\times\left(\frac{1}{3}e^{i\phi_M} - \frac{2M_\Delta\,\omega\,\alpha}{(3M_\Delta + m)(M_\Delta + m)}e^{i\phi_E}\right)\right\}. \tag{A14}$$

The isospin coefficients are defined as

$$C_\pi C_\gamma = \begin{cases} \pm\frac{\sqrt{2}}{3}, & \text{for } \pi^\mp, \\ \frac{2}{3}, & \text{for } \pi^0. \end{cases} \tag{A15}$$

The coupling constants G_1, G_3, the mass of the delta M_Δ and the width of the delta Γ_Δ were treated as parameters and fitted to the data. We use the following parametrization [21]

$$\begin{aligned} M_\Delta &= 1225 \text{ MeV}, \\ \Gamma_\Delta &= 110\left(\frac{|\mathbf{q}|}{|\mathbf{P}_a|}\right)^3 \frac{M_\Delta}{P_a} \frac{1+(0.007|\mathbf{P}_a|)^2}{1+(0.007|\mathbf{q}|)^2} \text{ MeV}, \\ G_1 &= 0.34\frac{M_\Delta + m}{m_\pi}, \\ G_3 &= 2.18/m_\pi \text{ MeV}^{-1}, \end{aligned} \tag{A16}$$

where $\mathbf{P}_a$ and $\mathbf{q}$ are in MeV/c and m_π is in MeV. The phases used to restore unitarity are functions of the variable $x = P_a - 1080$ in MeV and are given in degrees as

$$\begin{aligned} \phi_M &= -0.1228\sqrt{x} + 0.0735x, \\ \phi_E &= 3.9136\sqrt{x} + 0.2795x - 0.00049x^2. \end{aligned} \tag{A17}$$

The symbol α in Eq. (A14) is a constant that measures the relative strength between the $M1$ and $E2$ transition amplitudes in the Δ and here takes the value $\alpha = 0.8$, while $\omega = (P_a^2 - m^2)/(2P_a)$ is the photon energy in the π-N c.m. frame.

[1] *Perspectives on Photon Interactions with Hadrons and Nuclei*, Proceedings of the Workshop, edited by M. Schumacher and G. Tamas, Lecture Notes in Physics Vol. 365 (Göttingen, Germany, 1990).

[2] J. H. Koch, E. J. Moniz, and N. Ohtsuka, Ann. Phys. (N.Y.) **154**, 993 (1984); T. Suzuki, T. Takaki, and J. H. Koch, Nucl. Phys. **A460**, 607 (1986).

[3] G. S. Kyle *et al.*, Phys. Rev. Lett. **52**, 994 (1984); S. Gilad *et al.*, *ibid.* **57**, 2637 (1986); T. Takaki and M. Thies, Phys. Rev. C **28**, 2230 (1988).

[4] A. Nagl, V. Devanathan, and H. Überall, *Nuclear Pion Photoproduction* (Springer-Verlag, Berlin, 1991).

[5] C. Bennhold, L. Tiator, and L. E. Wright, Can. J. Phys. **68**, 1270 (1990).

[6] L. Tiator and L. E. Wright, Phys. Rev. C **30**, 989 (1984).

[7] L. Tiator, J. Vesper, D. Drechsel, N. Ohtsuka, and L. E. Wright, Nucl. Phys. **A485**, 565 (1988).

[8] M. K. Singham and F. Tabakin, Ann. Phys. (N.Y.) **135**, 71 (1981).

[9] K. Röhrich *et al.*, Nucl. Phys. **A475**, 762 (1987).

[10] L. Ghedira *et al.*, Phys. Rev. C **41**, 653 (1990).

[11] R. Wittman and N. C. Mukhopadhyay, Phys. Rev. Lett. **57**, 1113 (1986).

[12] R. C. Carrasco and E. Oset, Nucl. Phys. **A541**, 585 (1992).

[13] I. V. Glavanakov and V. N. Stibunov, Yad. Fiz. **30**, 897 (1979) [Sov. J. Nucl. Phys. **30**, 465 (1979)]; I. V. Glavanakov, *ibid.* **49**, 91 (1989) [**49**, 58 (1989)].

[14] I. V. Glavanakov, Yad. Fiz. **52**, 323 (1990) [Sov. J. Nucl. Phys. **52**, 205 (1990)].

[15] L. D. Pham *et al.*, Phys. Rev. C **46**, 621 (1992).

[16] G. van der Steenhoven, in Proceedings of the 7th Annual NIKHEF Conference, Amsterdam, 1991.

[17] J. M. Laget, Nucl. Phys. **A194**, 81 (1972).

[18] T. Suzuki, T. Takaki, and J. H. Koch, Nucl. Phys. **A460**, 607 (1986).

[19] L. B. Weinstein *et al.*, Phys. Rev. C **47**, 225 (1993).

[20] K. Hicks, spokesman, Proposal to the LEGS facility, 1992 (unpublished).

[21] K. I. Blomqvist and J. M. Laget, Nucl. Phys. **A280**, 405 (1977).

[22] J. M. Laget, Nucl. Phys. **A481**, 765 (1987).

[23] R. M. Davidson, N. C. Mukhopadhyay, and R. S. Wittman, Phys. Rev. Lett. **56**, 804 (1986).

[24] R. M. Davidson, N. C. Mukhopadhyay, and R. S. Wittman, Phys. Rev. D **43**, 71 (1991).

[25] S. Nozawa, B. Blankleider, and T.-S. H. Lee, Nucl. Phys. **A513**, 459 (1990); S. Nozawa, T.-S. H. Lee, and B. Blankleider, Phys. Rev. C **41**, 213 (1990).

[26] G. Blanpied *et al.*, Phys. Rev. Lett. **69**, 1880 (1992) and private communication with A. M. Sandorfi.

[27] K. Stricker, H. McManus, and J. A. Carr, Phys. Rev. C **19**, 929 (1979); **22**, 2043 (1980); **25**, 952 (1982).

[28] P. Schwandt *et al.*, Phys. Rev. C **26**, 55 (1982).

[29] S. S. Kamalov, L. Tiator, and C. Bennhold, Nucl. Phys. **A547**, 599 (1992).